\

Enzyme Immobilization on Metal Organic Frameworks: Laccase from *Aspergillus sp* is better adapted to ZIF-zni rather than Fe-BTC.

*Davide Tocco, [a,d] Cristina Carucci, [a,d]*Debora Todde,[a] Kim Shortall,[b] Fernando Otero,[b] Enrico Sanjust,[c,d] Edmond Magner,[b]* and Andrea Salis [a,d]**

a) Department of Chemical and Geological Sciences, University of Cagliari, and Centro NanoBiotecnologie Sardegna (CNBS), Cittadella Universitaria, SS 554 bivio Sestu, 09042, Monserrato (CA) (Italy)
b) Department of Chemical Sciences and Bernal Institute, University of Limerick, Limerick, V94 T9PX (Ireland)
c) Department of Biomedical Sciences, University of Cagliari, Cittadella Universitaria, SS 554 bivio Sestu, 09042 Monserrato (CA) (Italy)
d) Consorzio Interuniversitario per lo Sviluppo dei Sistemi a Grande Interfase (CSGI), via della Lastruccia 3, 50019, Sesto Fiorentino (FI), Italy. Unità Operativa University of Cagliari, Italy. Cittadella Universitaria, SS 554 bivio Sestu, 09042 Monserrato (CA), Italy

\

ABSTRACT

Laccase from *Aspergillus sp*. (LC) was immobilized within Fe-BTC and ZIF-zni metal organic frameworks through a one-pot synthesis carried out under mild conditions (room temperature and aqueous solution). The Fe-BTC, ZIF-zni MOFs, and the LC@Fe-BTC, LC@ZIF-zni immobilized LC samples were characterized by X-ray diffraction, scanning electron microscopy, Fourier transform infrared spectroscopy, and thermogravimetric analysis. The kinetic parameters (K_M and V_{max}) and the specific activity of the free and immobilized laccase were determined. Immobilized LCs resulted in a lower specific activity compared with that of the free LC (7.7 μmol min^{-1} mg^{-1}). However, LC@ZIF-zni was almost 10 times more active than LC@Fe-BTC (1.32 μmol min^{-1} mg^{-1} vs 0.17 μmol min^{-1} mg^{-1}) and only 5.8 times less active than free LC. The effect of enzyme loading showed that LC@Fe-BTC had an optimal loading of 45.2 mg g^{-1}, at higher enzyme loadings the specific activity decreased. In contrast, the specific activity of LC@ZIF-zni increased linearly over the loading range investigated. The storage stability of LC@Fe-BTC was low with a significant decrease in activity after 5 days, while LC@ZIF retained up to 50% of its original activity after 30 days storage. The difference in activity and stability between LC@Fe-BTC and LC@ZIF-zni is likely due to release of Fe^{3+} and the low stability of Fe-BTC MOF. Together, these results indicate that ZIF-zni is a superior support for the immobilization of laccase.

\

Introduction

Enzyme immobilization on solid supports has been widely explored.[1–3] Immobilized enzymes usually display high resistance to harsh environmental conditions and may exhibit improved thermal stability when compared to free enzymes. The enzymatic activity and stability depend on the choice of the support as well as on the method of immobilization.[1,4,5] A wide range of materials, e.g. mesoporous silica,[6–8] xerogels,[9] magnetic nanomaterials,[10] agarose,[11] liquid crystals,[12] nanofibrous polymers[13] and metal organic frameworks (MOFs) have been utilized for the immobilization of enzymes.[14–17] MOFs are composed of metal ions and organic linkers connected through coordination bonds to form a three-dimensional network.[18] They have been used for a range of applications, including storage of gases,[19] catalysis,[20] removal of pollutants,[21] biomedicine and sensing applications,[22,23] and, more recently, as enzyme supports.[24–26] In comparison with other supports, enzymes immobilized on MOFs can exhibit high catalytic activities, improved stability, and reusability.[27–29] Enzymes can be readily immobilized *in situ* in MOFs. Such *in situ* immobilization is facile, rapid and results in high enzyme loadings.[30] In this approach, enzyme molecules are entrapped in the three-dimensional network formed by the metal ions and the organic linkers. While a number of reports have focused on the catalytic activity of the immobilized enzymes, the spatial distribution has not been described in detail.[31,32] For example Liang et al.[33] tagged catalase (CAT) with fluorescein isothiocyanate (FITC) and used confocal laser scanning microscopy to show that the distribution and localization of the enzyme depended on the type of MOF used. A more homogeneous distribution was observed on MAF-7 and ZIF-90 in comparison to ZIF-8. Li et al.[34] immobilized cyt c and demonstrated that the protein was embedded in the Cu-BTC framework rather than within the pores. Finally, a number of enzymes can be co-immobilized within the same support.[35] However, the synthesis of MOF usually requires

\

long reaction times (several days for solvothermal and hydrothermal techniques and weeks for diffusion methods) and are often carried out under harsh conditions (high temperatures, use of organic solvents).[36] Such conditions are generally not appropriate for enzymes and result in denaturation and loss of catalytic activity. Recently, Gascón et al. immobilized different enzymes, e.g. alcohol dehydrogenase (ADH), glucose oxidase (GOx), and lipase in a basolite F300-like MOF using an *in situ* mild synthetic method.[37,38] This method involves entrapment of the enzyme within a MOF based on Fe^{3+} and the tridentate linker trimesic acid, in a process that is rapid and facile (room temperature and close to neutral pH). The synthesis occurs under mild conditions with the material displaying micro and meso-porous structure.[37] Similarly, Kida et al. developed a method to synthesize zeolite imidazole frameworks (ZIF-8) in aqueous solution[39] while Falcaro and co-workers immobilized several enzymes within a ZIF-8 material.[17] ZIF-zni is a robust, dense, non-porous material.[40,41] ZIF-zni, one of the most stable MOF materials, is usually synthetized at very high temperatures and in organic solvents.[40] Nevertheless, it can be also be prepared at room temperature, using water as the solvent.[42]

Laccases (LCs, E.C. 1.10.3.2, p-diphenol: dioxygen oxidoreductase), are multicopper oxidases that catalyze the oxidation of various phenolic and non-phenolic compounds[43] via reduction of molecular oxygen to water.[44] In addition to p-diphenols (quinols), o-diphenols (catechols), alkoxyphenols and their derivatives, aromatic amines and aminophenols can also act as substrates for laccase. Due to their strong electron-rich character, nonphenolic substrates such as polymethoxybenzenes[45] can act as substrates for laccases. The radical products produced in the catalytic reaction are particularly favored when the lone electron can be efficiently delocalized in the aromatic systems, forming semiquinones, with further reaction depending on the properties of the products, pH and the concentration of oxygen. In nature, laccases (LCs) are present in plants,

\

bacteria, insects and white rot fungi.[46,47] Due to their low substrate specificity, LCs are used for a wide range of applications, such as bleaching of denim and paper,[48] removal of toxicants released during combustion processes,[49] decolorisation,[50] elimination of phenolics,[6] and biomass delignification.[51–53] Recently Naseri et al. immobilized laccase from *Trametes versicolor* on ZIF-zni and ZIF-8, two different zeolite imidazolate frameworks, to study enzymatic activity and stability to storage and recycling.[54] Li et al. encapsulated laccase (*Ganoderma lucidum*) in ZIF-8 to form an enzymatic biofuel cell based self-powered biosensor.[22] Gascon et al. compared the immobilization of laccase (*Aspergillus oryzae*) on Fe-BTC MOF obtained through a one-pot and a post-synthesis method, and also investigated the catalytic activity and enzyme leaching.[55] Although laccases are very useful enzymes for a wide range of applications,[44,56] they possess low stability in their soluble form, being easily perishable at neutral and basic pH.[57] Moreover, when immobilized on solid supports, the catalytic activity and stability of laccases is strongly affected by the amount of water present in the preparation, indeed the activity and stability rapidly decrease upon drying.[58]

The majority of reports on the immobilization of enzymes on MOFs focus on single MOF materials, describing the immobilization of different enzymes in the MOF[38,59,60] to demonstrate the potential use of a specific MOF support. This study compares two different MOF materials as supports for the *in situ* immobilization of *Aspergillus sp.* laccase. More specifically, laccase (LC) was entrapped within Fe-BTC MOF and ZIF-zni, to obtain LC@Fe-BTC and LC@ZIF-zni biocatalysts[38,54](Scheme 1). The properties of the immobilized biocatalysts were extensively characterized, and the kinetic parameters, K_M and V_{max} compared with those of the free laccase. Specific activities for different laccase loadings were measured, together with the storage stability.

\

This study enabled a detailed comparison of *in situ* enzyme immobilization on the two MOF supports, Fe-BTC and ZIF-zni.

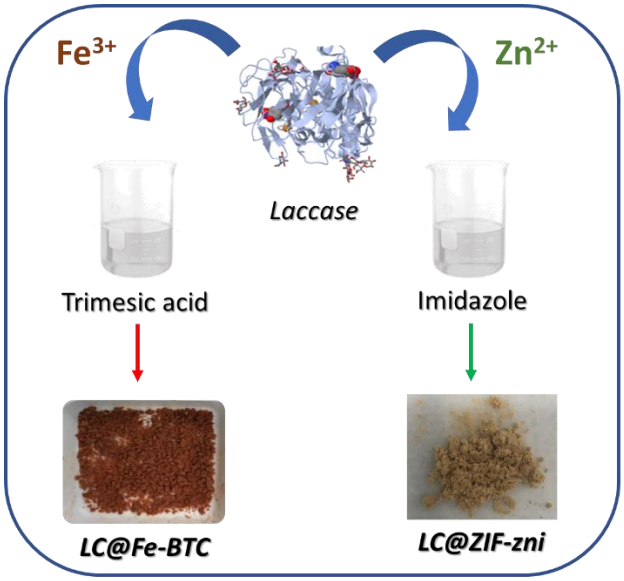

Scheme 1. Synthesis and immobilization of LC in ZIF-zni and Fe-BTC supports

Results and Discussion

Characterisation of Fe-BTC, LC@Fe-BTC, ZIF-zni and LC@ZIF-zni samples

Fe-BTC and ZIF-zni and laccase modified MOFs (LC@Fe-BTC and LC@ZIF-zni) were characterised using X-ray diffraction. The XRD patterns (Fig. 1A) show sharp peaks at 11°, 19°, 24°, 28°, and 34° confirming the formation of the Fe-BTC structure.[37,61,62] Fig. 1B confirms the formation of the ZIF-zni materials, with characteristic peaks at 15°, 17°, 18°, 21° in agreement with previous literature reports.[14,63] The XRD patterns obtained for both LC@Fe-BTC and LC@ZIF-zni samples do not differ significantly from those of Fe-BTC and ZIF-zni demonstrating that laccase does not significantly alter the structure of the MOFs. Thermogravimetric analysis (TGA) demonstrated that Fe-BTC MOF had a loss of mass of 12% over the range 0-115°C, while

\

LC@Fe-BTC showed a much higher loss of up to 35% over the same temperature range. These losses can be attributed to different amounts of adsorbed water in the samples.[55] Fe-BTC MOF showed a loss of 14.5% over the range 115-330°C and of 43% over the range 330-500°C, with the latter likely due to the decomposition of the Fe-BTC structure. In contrast to Fe-BTC, the LC@Fe-BTC sample did not show a clear loss in mass at 330°C, as confirmed by the derivative plot (dm/dT vs T, Fig. S1). Enzyme immobilization thus shifted the thermal decomposition of the MOF to higher temperatures. For LC@Fe-BTC samples, the mass loss over the temperature range 115-430°C is likely due to the decomposition of BTC and of LC encapsulated in the support. However, the exact mass loss due to the enzyme decomposition cannot be quantified as it overlaps that of trimesic acid (Fig. 1C).[64] Finally, the mass loss measured above 430°C for LC@Fe-BTC is assigned to the decomposition of the MOF structure.[65] Thermogravimetric analysis of ZIF-zni and LC@ZIF-zni (Fig. 1D) shows that the materials exhibited good thermal stability in air, up to 433°C, in agreement with literature reports.[66] ZIF-zni had mass losses of 10 and 25% over the ranges, 433-566°C and 566-700°C. The first mass loss can be attributed to the partial loss of ZIF crystallinity which is favoured in oxidizing environments[67] while the latter can be ascribed to the complete decomposition and collapse of the ZIF-zni structure.[68] Thermogravimetric analysis of LC@ZIF-zni was comparable with ZIF-zni except for the mass loss of 13 % over the temperature range, 245-400°C. ZIF-zni displayed a loss in mass of 2.8 % over this range, indicating that loss in mass of LC@ZIF-zni could be ascribed to the thermal decomposition of immobilized laccase (Table S1).

\

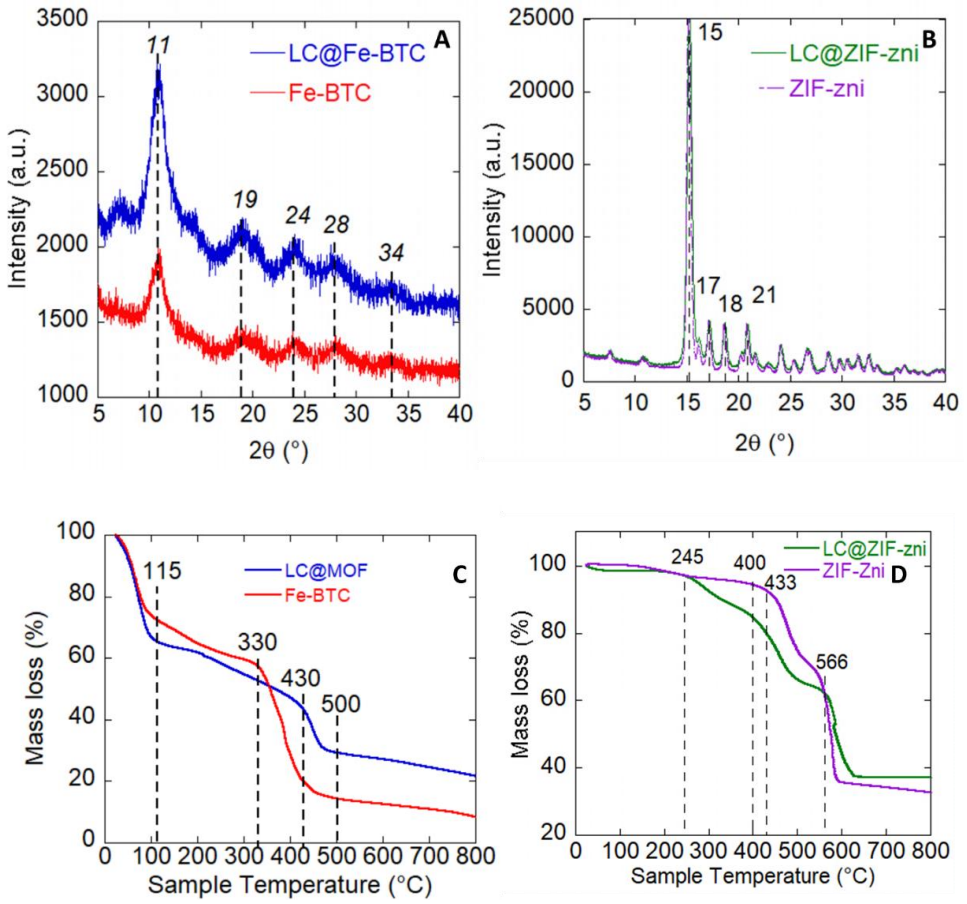

Figure 1. XRD patterns of a) Fe-BTC and LC@Fe-BTC and b) ZIF-zni and LC@ZIF-zni. Thermogravimetric analysis (TGA) curve from 25 °C to 800 °C of c) Fe-BTC MOF and LC@Fe-BTC 45.2 mg g^{-1} and d) ZIF-zni and LC@ZIF-zni 84 mg g^{-1}.

Scanning electron microscopy (SEM) images (Fig. 2 A-B) of Fe-BTC show agglomerates of irregular particles and are similar to literature reports.[69] SEM images (Fig. 2 C-D) of ZIF-zni show a more regular crystalline morphology. LC@Fe-BTC samples have a more irregular particle shape, likely due to enzyme immobilization (Fig. 2 B). Similar to immobilization in ZIFs, encapsulation of laccase in Fe-BTC led to changes in particle morphology, in which the particles lose their regular shape in favor of more disordered agglomerates, in agreement with other reports on the immobilization of enzymes such as lipase, glucose oxidase and alcohol dehydrogenase.[30,38]

\

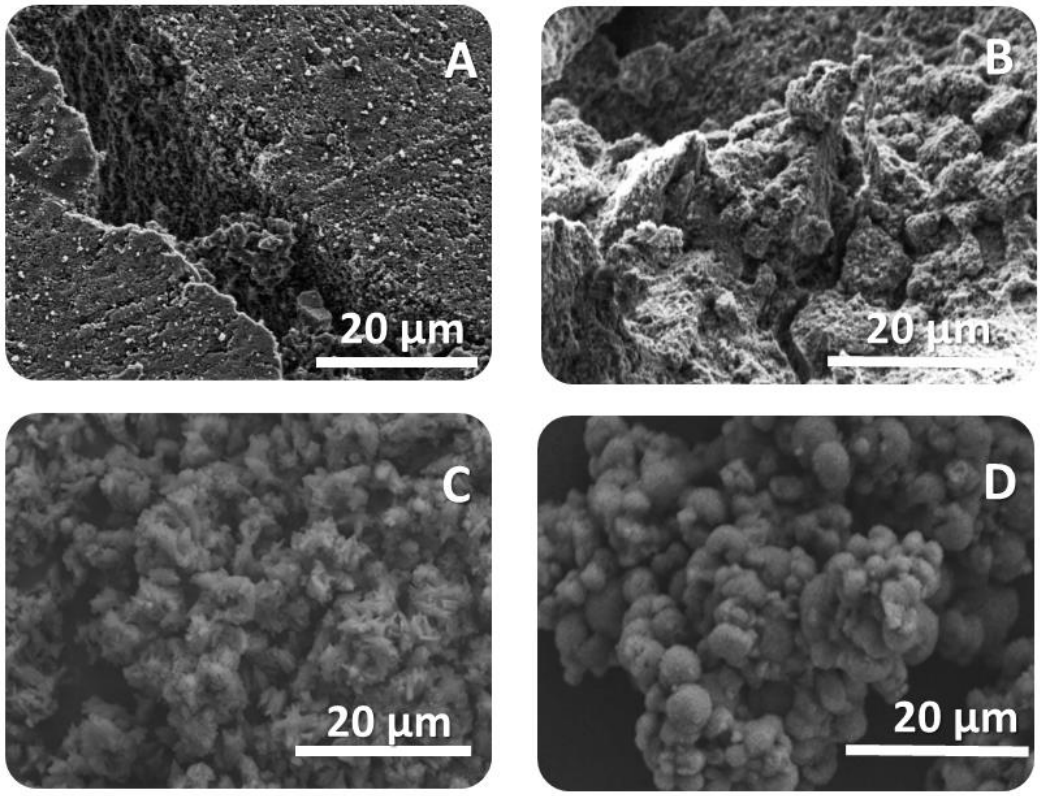

Figure 2. SEM images of A-B) Fe-BTC and LC@Fe-BTC C-D) ZIF-zni and LC@ZIF-zni samples

The FTIR spectrum of Fe-BTC (Fig. 3A) showed a band above 3300 cm^{-1} assigned to OH stretching, indicative of the presence of adsorbed water. The peak at 1625 cm^{-1} can be attributed to the C=O stretching of carboxylate groups.[65] The peaks, arising from the carboxylate groups of trimesic acid, likely mask the NH-C=O amide bands of the protein. The bands at 1447 cm^{-1} and 1375 cm^{-1} are due to asymmetric and symmetric stretching of the O-C-O group, respectively.[70] The other two sharp peaks at 750 and 703 cm^{-1} correspond to the bending of aromatic C–H bonds.[61,71] FTIR spectra of ZIF-zni and LC@ZIF-zni samples are shown in Fig. 3C and 3D. The bands in the range of 600 - 1500 cm^{-1} are ascribed to the stretching and bending modes of the

\

imidazole ring.[72] The presence of imidazole bands obscures the amide band expected for the enzyme.

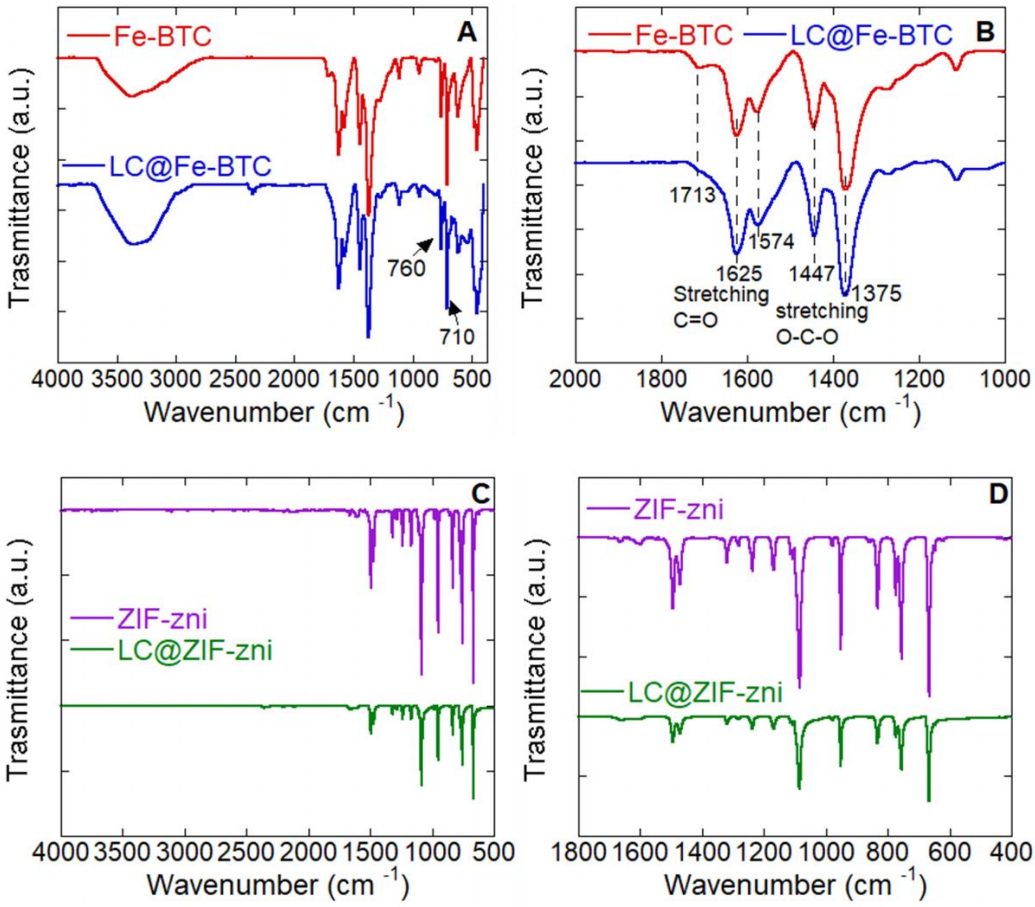

Figure 3. FT-IR spectrum of a) Fe-BTC wavenumber range from 450 to 4000 cm^{-1} b) LC@Fe-BTC wavenumber range from 1000 to 1800 cm^{-1} and c) ZIF-zni wavenumber range from 500 to 4000 cm^{-1} d) LC@ZIF-zni wavenumber range from 400 to 1800 cm^{-1}.

In particular, the sharp peaks in the range 1100 - 1400 cm^{-1} region are attributed to the C=N stretching.[73] The peak at 668 cm^{-1} is due to the stretching of the Zn–N coordination bond between Zn and the imidazole ring.[74] The presence of laccase was confirmed by EDX measurements with 0.14 and 0.20% (m/m) of copper for LC@Fe-BTC and LC@ZIF-zni (Figure S8), respectively, in agreement with the ratio of laccase loadings for both materials.

\

A wide range of studies have been described on the use of iron based MOFs,[75] but their long term stability, especially of Fe-BTC, has not been studied in detail. Oveisi et al. reported leaching of 0.3 ppm of Fe^{2+} (0.01% of the initial amount) in the synthesis of Fe-BTC MOF.[76] Sanchez et al. reported similar negligible amounts of iron leaching (0.3 ppm).[37] Aguilar et al. studied the hydroxylation of phenol using Fe-BTC. Fe leaching was absent or negligible at room temperature but increased with temperature up to 26 ppm at 50 °C.[77] A study demonstrated how nanoparticles of MIL-100 progressively lose their crystallinity when incubated in PBS (phosphate buffer saline) solution from 6 h to 3 days due to the interaction between phosphate and iron ions.[78] Similarly to MIL-100, Fe-BTC is unstable in aqueous buffer solutions. Determination of iron release from Fe-BTC was analyzed following a SCN^- based colorimetric assay (Figure S6). Iron release was assayed by suspending Fe-BTC in citrate, phosphate and Tris-HCl buffers (10 and 100 mM) at pH 5, 7 and 9, respectively under static and shaking conditions for 24 and 48 h (Figure S7). Samples suspended in 10 mM buffer in shaking conditions demonstrated a higher concentration of iron release (up to 35 μM at pH 5 and 9 after 48 h) than samples stored in static conditions (up to 25 μM at pH 5 after 24 and 48 h). In 100 mM buffer solutions, samples at pH 5 showed comparable leaching levels of iron (25 μM) with no significant differences between static and shaking conditions and between 24 and 48 h of storage. Samples stored at pH 7 and 9 demonstrated an increase in iron release up to 40 μM after 48 h. The increased amounts of iron released in 100 mM buffer indicates that the buffer concentration is a factor in the stability of the material. Overall, the data demonstrate that Fe-BTC is unstable upon exposure to aqueous buffer, limiting its use as a support for enzymes. A comparable systematic study of ZIF-8 stability in PBS demonstrated that ZIF-8 is unstable and releases metal ions in the presence of specific buffer solutions.[79] In that work Falcaro et al. demonstrated that ZIF-8 particles can rapidly lose crystallinity when incubated in

\

PBS for 1 h to 24 h, leading to the formation of zinc phosphate particles with the rate of degradation depending on the size of the ZIF-8 particles. In another work, Gassensmith et al. demonstrated that ZIF-8 is more stable in some buffers and cell media.[80] The stability of ZIF-8 stability is dependent on the stability of the bond between Zn^{2+} and 2-methylimidazole linker. Both phosphate and bicarbonate can bind to Zn^{2+} competing with the linker and reducing the stability of the material. The stability of ZIF-8 was assessed by examining the surface morphology, degree of crystallinity of the material and leaching of the protein. No significant leaching of protein or changes in crystallinity were observed indicating that ZIF-8 is stable in the buffers used.

SEM and XRD were used to evaluate the structural stability of LC@Fe-BTC and LC@ZIF-zni after use (Figure S10-S11). While the XRD pattern of LC@ZIF-zni displayed more noise and was more irregular, the main peaks (2θ peak position: 10, 15, 18, 20) were retained indicative of a partial loss of the MOF structure. SEM images confirmed that the surface morphology was not significantly changed (Figure S11). The XRD pattern of Fe-BTC is not well defined due to the semi-amorphous nature of the material. The XRD patterns before and after use were similar (Figure S10) As with LC@ZIF-zni, SEM images confirmed that there were no substantial changes in the morphology of LC@Fe-BTC after use (Figure S11).

The effect of immobilization on kinetic properties

Figure 4 shows the kinetic data obtained for the free and immobilized laccases, while the associated kinetic parameters are listed in Table 1. The laccase from *Aspergillus sp*. used in this work showed a 45-fold loss in specific activity once immobilized within Fe-BTC (from 7.7 to 0.17 μmol min^{-1} mg^{-1}). Gascón et al.[55] reported the immobilization of a laccase from *Aspergillus oryzae* within Fe-BTC. Their results showed a 95-fold decrease in catalytic activity (from 378 to 4 μmol min^{-1} mg^{-}

\

^{1}) when the laccase was entrapped in Fe-BTC. With LC@ZIF-zni, a much lower decrease in activity, by a factor of 5.8, was observed (V_{max} decreased from 7.7 to 1.32 μmol min^{-1} mg^{-1}).

Table 1. Kinetic parameters obtained with free laccase, LC@MOF and LC@ZIF-zni samples.

Samples	K_m (μM)	V_{max} (μmol min^{-1} mg^{-1})
Free laccase	13 ± 3	7.7 ± 0.4
LC@Fe-BTC	35 ± 7	0.17 ± 0.01
LC@ZIF-zni	22 ± 6	1.32 ± 0.08

The decrease in V_{max} observed with both supports may be due to diffusional limitations or, alternatively to enzyme inactivation. LC@Fe-BTC showed an increase in K_M (2.7 times higher than free laccase) suggesting that the substrate had a lower affinity for the enzyme when immobilized on Fe-BTC. LC@ZIF-zni sample showed an increase in K_M (x 1.6) compared with the free enzyme. Differences in the kinetic parameters frequently arise upon immobilization of an enzyme.[81] Differences in kinetic parameters between free and immobilized enzymes can arise from a range of factors that include changes in conformation, in the structure or degree of accessibility of the enzyme's active site, in the rate of diffusion and/or in partitioning of the substrate to the active site.[82] Similar to the results described here, Patil et al., immobilized laccase from *Trametes hirsuta* in ZIF-8 and reported a 1.5 fold increase in K_M, and a 1.2 fold decrease in V_{max} suggesting that the ZIF materials may be suitable supports for the immobilization of laccase.[83] Some enzymes such as catalase showed a decrease in catalytic activity upon immobilization on ZIF-8.[33] This was ascribed to the hydrophobic nature of ZIF-8 that may interact with hydrophobic residues of the enzyme. In another work, lipase (*Candida antarctica B*) was immobilized on Fe-BTC with no significant loss of enzymatic activity.[55] On the other hand, when laccase (*Aspergillus oryzae*) was

\

immobilized on the same material, the activity decreased (up to 0.2 µmol min^{-1} mg^{-1}), thus suggesting that Fe-BTC was not a good host for the enzyme.[55]

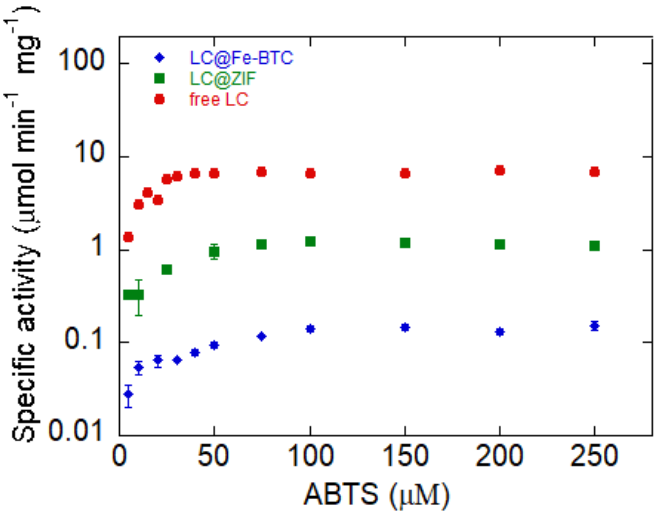

Figure 4. Michaelis-Menten plots of the activity of of free laccase, LC@Fe-BTC (9 mg mL^{-1}) and LC@ZIF-zni (9 mg mL^{-1}).

Effect of enzyme loading on specific activity

Different LC@Fe-BTC and LC@ZIF-zni samples with increasing protein loading were prepared using enzyme concentrations in the range 6-10 mg mL^{-1} (LC@Fe-BTC) and 5-12.5 mg mL^{-1} (LC@ZIF-zni) during the *in situ* immobilization process. LC@Fe-BTC loadings, quantified by means of the Bradford assay, varied from 29.8 mg g^{-1} to 52.7 mg g^{-1} (Figure 5A; Table S1) while LC@ZIF-zni loadings ranged from 17.8 mg g^{-1} to 59.5 mg g^{-1} (Figure 5C; Table S2). The immobilization efficiency (IE%), defined as the ratio (%) between the amount of immobilized protein and the total protein in solution, was 100 % for all LC@Fe-BTC samples, demonstrating that all of the laccase was immobilized within Fe-BTC material. When LC@ZIF-zni was analyzed, IE% varied between 97-99 % for all samples showing, also in this case, a very high immobilization efficiency. For LC@Fe-BTC samples, the increase in enzyme loading shown in Fig. 5A is

\

supported by TGA analysis (Fig. 5B). TGA analysis of LC@Fe-BTC samples (6 and 7 mg/mL) displayed a loss in mass of 70% over the range 0 and 115 °C due to the loss of water. At higher enzyme concentrations (9 and 10 mg/mL). LC@Fe-BTC samples had losses in mass of 25%, likely due to a lower water content. The % mass loss in the range 115 - 430°C increased with increasing enzyme loading from 9.5% to 22%, with the exception of LC@Fe-BTC with a loading of 45.2 mg g^{-1} that showed a mass loss of 27%. TGA curve for Fe-BTC did not show any mass losses in the range between 200 and 300 °C. On the other hand, in the same temperature range LC@Fe-BTC samples showed a low mass loss (more visible in the derivative curve, Fig. S1) that increased with increasing enzyme loading. Gascón et al. investigated the mass loss of enzymes immobilized within Fe-BTC MOF through thermogravimetric analysis coupled to mass spectrometry.[55] In that work, they attributed the mass loss over the temperature range 200 - 300°C to water retained by the enzyme.[55] LC@ZIF-zni samples showed a linear increase in mass loss in the temperature range 245-400°C except for the loading at 19.8 mg g^{-1} that showed a mass loss of 9.5 % (Table S2).

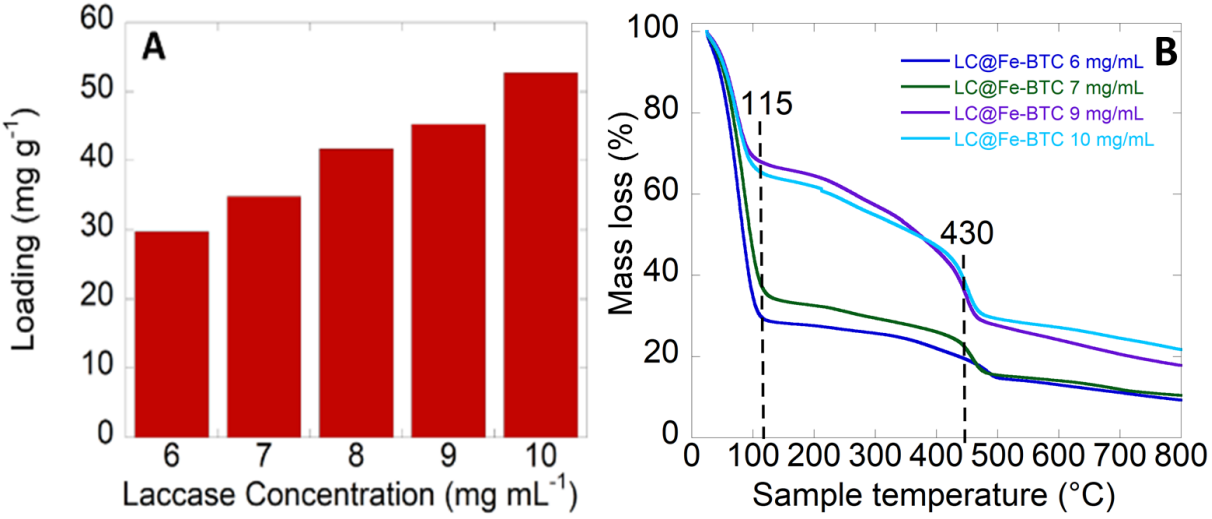

\

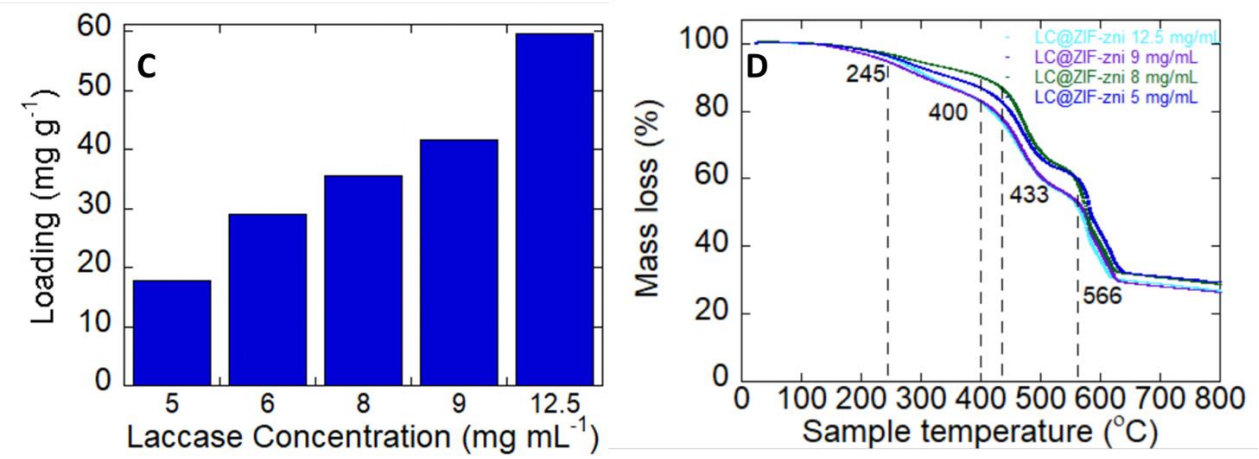

Figure 5. a) Protein loading of Fe-BTC MOF, b) thermogravimetric analysis (TGA) of LC@Fe-BTC with different enzyme loadings c) Protein loading of ZIF-zni samples d) thermogravimetric analysis (TGA) of LC@ZIF-zni with different enzyme loadings

Specific activity of LC@Fe-BTC and LC@ZIF-zni

The specific activities of the samples at different enzyme loadings were examined. In the absence of diffusional limitations, the activity should increase as the loading is increased. Figure 6 shows an initial linear increase in activity with enzyme loading on LC@Fe-BTC up to an activity of 0.08 units to at a loading of 45.2 mg g^{-1}. Above this loading the specific activity decreased, likely arising from limitations in substrate diffusion within the pores[6,84] For the loadings examined, the specific activity is an order of magnitude higher for ZIF-zni samples than Fe-BTC biocatalysts. In contrast, with LC@ZIF-zni an increase in activity over the range investigated (Fig. 6), was observed, indicating diffusional limitations were not observed. Naseri et al.[54] obtained a high retention of activity of a laccase from *T. versicolor* in ZIF-zni demonstrating a very high adaptability of laccases for ZIF-zni support. The laccase from *Aspergillus sp*. is a glycoprotein containing about 10% sugar content.[44,85] The presence of asparagine-N-linked sugar residues on the enzyme confer polar, hydrophilic properties on the enzyme.

\

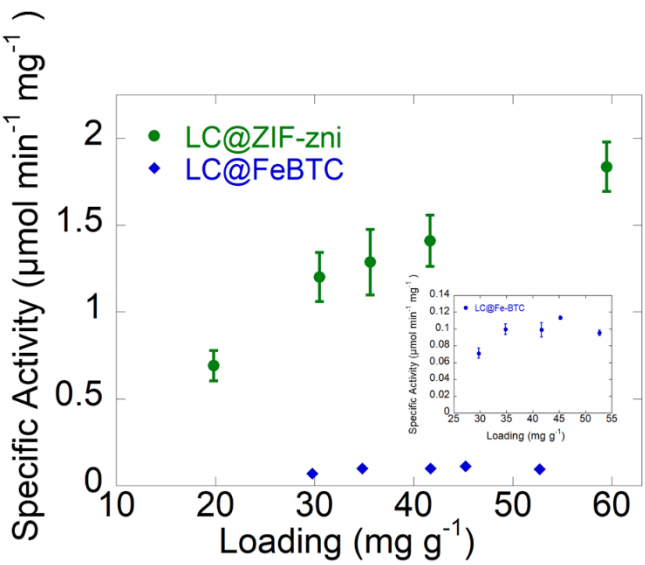

Figure 6. Effect of loading on specific activity of LC@Fe-BTC and LC@ZIF-zni. Inset: enlargement of data for LC@Fe-BTC

As studied recently by Liang et al., the enzyme polarity is likely related to high activity retention in ZIF materials.[33] Likely, ZIF-zni materials offer a more favorable environment for laccase activity in comparison with Fe-BTC supports. When Knedel et al.[16] immobilized laccase from *Corynebacterium glutamicum* in ZIF-8, no activity was observed when ABTS was used as the substrate. The lack of activity was explained on the basis that the small ZIF-8 pore windows (3.4 Å) which did not allow ABTS to enter the pores and reach the enzyme active site. Liang et al. demonstrated how, even in porous ZIFs, ca. 40% of the enzyme was on the surface rather than entrapped in the material.[42]

Knedel at al. also reported how laccase immobilization in ZIF materials using 2,6-dimethoxyphenol and syringaldazine substrates enhanced stability in ethanol and N,N-dimethlyformamide (DMF)[16] meaning that, upon immobilization in ZIF-8, laccase works also in the absence of water. When laccase is immobilized in chitosan the laccase water requirement decreased up to 7% in water content.[86] In our work, the relative amount of water present in the Fe-BTC and ZIF-zni samples can be seen by the differential scanning calorimetry (DSC) plot. A small

\

endothermic (positive) peak between 100 and 200 °C can be attributed to water retained in ZIF-zni samples (Fig. S3). Over the temperature range 80-130 °C, a much bigger endothermic peak was seen for Fe-BTC samples (Fig. S4) indicative of a higher water content. As shown in Figure 5B-D, from TGA data, LC@ZIF-zni resulted in dryer samples for all the assayed loadings in comparison with LC@Fe-BTC samples. In principle, drying of the immobilized biocatalyst should result in a significant decrease in laccase activity.[6] In fact, LC@ZIF-zni retained higher activities at various enzymatic loadings even if samples with reduced moisture content (1 % vs 35 % in water content for biocatalyst with 59.4 and 52.7 mg/g of enzymatic loading for ZIF-zni and Fe-BTC respectively) than Fe-BTC were used (Fig. 5D). It is worth noticing that also at the optimal Fe-BTC loadings, LC@ZIF-zni displayed a 10-fold higher activity than LC@Fe-BTC (1.32 μmol min^{-1} mg^{-1} *vs* 0.17 μmol min^{-1} mg^{-1}) indicative of a superior immobilization environment in ZIF-zni when compared to Fe-BTC .

Storage stability of LC@Fe-BTC and LC@ZIF-zni

Samples of LC@Fe-BTC and LC@ZIF-zni were stored at 4 °C and the residual activity was checked every 3-5 days. The storage stability of LC@Fe-BTC showed a rapid linear decrease, retaining only 16% of initial activity (0.59 ± 0.11 μmol min^{-1} g^{-1}) after eight days, while LC@ZIF-zni retained 82% of its initial activity (8.18 ± 0.14 μmol min^{-1} g^{-1}). On comparison of the two supports there was over 60% difference in retention of activity, confirming that ZIF-zni is a superior support. Furthermore, LC@ZIF-zni retained about 50% of its initial activity at the 30th day. The rapid decrease in LC activity may be due to enzyme denaturation in the Fe-BTC material, but the lower stability of the Fe-BTC material is likely a significant factor. Good retention of catalytic activity in ZIF materials was reported by Ulu who described the immobilization of asparaginase in ZIF-8[87] with the immobilized enzyme retaining 40% of initial activity after four

\

weeks, similar to the data described here. The stability of laccase (*Trametes hirsute*) immobilized on ZIF-8 was described by Patil et al.[83] with only 20% loss of activity after storage for 20 days at 30°C. The good storage stability of laccase in ZIF-zni highlights its possible use as a support for laccase immobilization.

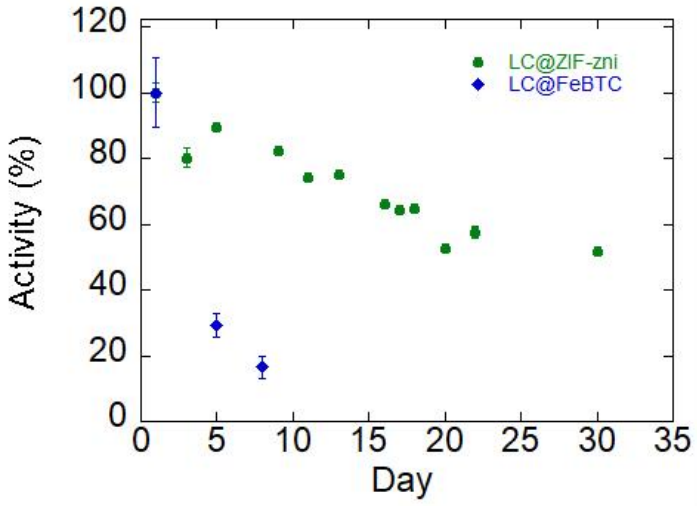

Figure 7. Storage stability of LC@Fe-BTC and LC@ZIF-zni, activity normalized at 3.6 and 13.7 μmol min^{-1} g^{-1} respectively.

Reuse is an important aspect in evaluating immobilized enzymes. Samples of LC@Fe-BTC and LC@ZIF-zni were evaluated for reuse. (Figure S9). ZIF-zni samples showed a rapid decrease after use, with a residual activity of 6.2 % after three cycles. On the contrary, Fe-BTC displayed a significantly better performance retaining 18.2% activity after the 10^{th} cycle. The rapid decrease in activity of the ZIF-zni samples is likely due to practical difficulties in recovering the samples as the crystal size of the ZIF biocatalysts dissolve when in contact with some buffers making its recover and reuse very challenging. A similar phenomenon was recently observed by Maddigan et al. [88]

\

Conclusions

The comparison between two MOF materials used for the *in situ* immobilization of *Asperigillus sp.* laccase was described. The structures of both supports were characterized using XRD, SEM, TGA and FTIR techniques. Immobilization efficiency was 100% for all LC@Fe-BTC loadings while for ZIF samples it was slightly lower (from 97-99 %). Surprisingly, LC@ZIF-zni showed a much higher V_{max} when compared with LC@Fe-BTC samples. The K_M value of LC@ZIF-zni is lower (21.6 μM) than that of LC@Fe-BTC (35.5 μM) suggesting more efficient substrate binding by laccase in ZIF-zni. The enzymatic activities were studied in a wide range of loadings. In the case of Fe-BTC samples, a maximal specific activity was observed at an optimal loading of 42.5 mg g^{-1} whereas higher loadings resulted in a specific activity decrease. Differently, LC@ZIF-zni samples did not show any decrease in activity up to 59.4 mg g^{-1} indicating that a higher amount of laccase can be immobilized without observed limitations. Lastly, the storage stability of both immobilized biocatalysts was studied indicating a much higher activity retention for LC@ZIF-zni samples (50% loss of initial activity after 30 days) than LC@Fe-BTC (84% loss of initial activity after 8 days). ZIF-zni material is a promising material for the *in situ* immobilization of laccase with good retention of activity while Fe-BTC materials do not possess long term stability.

Corresponding Author

*Dr. Cristina Carucci cristina.carucci@unica.it, *Prof. Andrea Salis asalis@unica.it, *Prof. Edmond Magner edmond.magner@unica.it

Author Contributions

The manuscript was written through contributions of all authors. All authors have given approval to the final version of the manuscript.

\

Funding Sources

Any funds used to support the research of the manuscript should be placed here (per journal style).

ACKNOWLEDGMENT

DT thanks Erasmus+ and MIUR (PON RI 2014-2020, Azione l.1 "Dottorati Innovativi con Caratterizzazione industriale"- DOT1304455 2) for financing his PhD scholarship. CC gratefully acknowledges MIUR (PON-AIM Azione I.2 – DD n. 407-27.02.2018, AIM1890410 - 2). AS gratefully thanks financial support from FIR 2020, and MIUR (FFABR 2017). We wish to acknowledge the assistance of Dr. Wynette Redington (XRD characterization) and of Denise Demurtas and Simin Arshi (SEM and EDX characterization).

REFERENCES

(1) Magner, E. Immobilisation of Enzymes on Mesoporous Silicate Materials. *Chem. Soc. Rev.* **2013**, *42* (15), 6213–6222. https://doi.org/10.1039/c2cs35450k.

(2) Basso, A.; Serban, S. Industrial Applications of Immobilized Enzymes—A Review. *Mol. Catal.* **2019**, *479* (March), 110607. https://doi.org/10.1016/j.mcat.2019.110607.

(3) Molina, F.; Rueda, A.; Bosque-Sendra, J. M.; Megías, L. Determination of Proteins in the Presence of Imidazole Buffers. *J. Pharm. Biomed. Anal.* **1996**, *14* (3), 273–280. https://doi.org/10.1016/0731-7085(95)01615-5.

(4) Hanefeld, U.; Gardossi, L.; Magner, E. Understanding Enzyme Immobilisation. *Chem. Soc. Rev.* **2009**, *38* (2), 453–468. https://doi.org/10.1039/B711564B.

\

(5) Sheldon, R. A.; van Pelt, S. Enzyme Immobilisation in Biocatalysis: Why, What and How. *Chem. Soc. Rev.* **2013**, *42* (15), 6223–6235. https://doi.org/10.1039/c3cs60075k.

(6) Salis, A.; Pisano, M.; Monduzzi, M.; Solinas, V.; Sanjust, E. Laccase from Pleurotus Sajor-Caju on Functionalised SBA-15 Mesoporous Silica: Immobilisation and Use for the Oxidation of Phenolic Compounds. *J. Mol. Catal. B Enzym.* **2009**, *58* (1–4), 175–180. https://doi.org/10.1016/j.molcatb.2008.12.008.

(7) Pitzalis, F.; Monduzzi, M.; Salis, A. A Bienzymatic Biocatalyst Constituted by Glucose Oxidase and Horseradish Peroxidase Immobilized on Ordered Mesoporous Silica. *Microporous Mesoporous Mater.* **2017**, *241*, 145–154. https://doi.org/10.1016/j.micromeso.2016.12.023.

(8) Piras, M.; Salis, A.; Piludu, M.; Steri, D.; Monduzzi, M. 3D Vision of Human Lysozyme Adsorbed onto a SBA-15 Nanostructured Matrix. *Chem. Commun.* **2011**, *47* (26), 7338–7340. https://doi.org/10.1039/c1cc11840d.

(9) Fernandez Caresani, J. R.; Dallegrave, A.; dos Santos, J. H. Z. Amylases Immobilization by Sol–Gel Entrapment: Application for Starch Hydrolysis. *J. Sol-Gel Sci. Technol.* **2020**, *94* (1), 229–240. https://doi.org/10.1007/s10971-019-05136-7.

(10) Wastewater, T.; Siddeeg, S. M.; Tahoon, M. A.; Mnif, W. Iron Oxide / Chitosan Magnetic Nanocomposite Immobilized Manganese Peroxidase For.

(11) Zucca, P.; Fernandez-Lafuente, R.; Sanjust, E. Agarose and Its Derivatives as Supports for Enzyme Immobilization. *Molecules* **2016**, *21* (11), 1577. https://doi.org/10.3390/molecules21111577.

\

(12) Valldeperas, M.; Salis, A.; Barauskas, J.; Tiberg, F.; Arnebrant, T.; Razumas, V.; Monduzzi, M.; Nylander, T. Enzyme Encapsulation in Nanostructured Self-Assembled Structures: Toward Biofunctional Supramolecular Assemblies. *Curr. Opin. Colloid Interface Sci.* **2019**, *44*, 130–142. https://doi.org/10.1016/j.cocis.2019.09.007.

(13) Temoçin, Z.; İnal, M.; Gökgöz, M.; Yiğitoğlu, M. Immobilization of Horseradish Peroxidase on Electrospun Poly(Vinyl Alcohol)–Polyacrylamide Blend Nanofiber Membrane and Its Use in the Conversion of Phenol. *Polym. Bull.* **2018**, *75* (5), 1843–1865. https://doi.org/10.1007/s00289-017-2129-5.

(14) Pitzalis, F.; Carucci, C.; Naseri, M.; Fotouhi, L.; Magner, E.; Salis, A. Lipase Encapsulation onto ZIF-8: A Comparison between Biocatalysts Obtained at Low and High Zinc/2-Methylimidazole Molar Ratio in Aqueous Medium. *ChemCatChem* **2018**, *10* (7), 1578–1585. https://doi.org/10.1002/cctc.201701984.

(15) Zhong, L.; Feng, Y.; Wang, G.; Wang, Z.; Bilal, M.; Lv, H.; Jia, S.; Cui, J. Production and Use of Immobilized Lipases in/on Nanomaterials: A Review from the Waste to Biodiesel Production. *Int. J. Biol. Macromol.* **2020**, *152*, 207–222. https://doi.org/10.1016/j.ijbiomac.2020.02.258.

(16) Knedel, T. O.; Ricklefs, E.; Schlüsener, C.; Urlacher, V. B.; Janiak, C. Laccase Encapsulation in ZIF-8 Metal-Organic Framework Shows Stability Enhancement and Substrate Selectivity. *ChemistryOpen* **2019**, *8* (11), 1337–1344. https://doi.org/10.1002/open.201900146.

(17) Liang, K.; Ricco, R.; Doherty, C. M.; Styles, M. J.; Bell, S.; Kirby, N.; Mudie, S.; Haylock,

\

D.; Hill, A. J.; Doonan, C. J.; Falcaro, P. Biomimetic Mineralization of Metal-Organic Frameworks as Protective Coatings for Biomacromolecules. *Nat. Commun.* **2015**, *6*, 4–11. https://doi.org/10.1038/ncomms8240.

(18) Wu, X.; Hou, M.; Ge, J. Metal–Organic Frameworks and Inorganic Nanoflowers: A Type of Emerging Inorganic Crystal Nanocarrier for Enzyme Immobilization. *Catal. Sci. Technol.* **2015**, *5* (12), 5077–5085. https://doi.org/10.1039/C5CY01181G.

(19) Gulati, A.; Kakkar, R. DFT Studies on Storage and Adsorption Capacities of Gases on MOFs. *Phys. Sci. Rev.* **2018**, *3* (8). https://doi.org/10.1515/psr-2017-0196.

(20) Van Nguyen, C.; Matsagar, B. M.; Yeh, J.-Y.; Chiang, W.-H.; Wu, K. C. W. MIL-53-NH2-Derived Carbon-Al2O3 Composites Supported Ru Catalyst for Effective Hydrogenation of Levulinic Acid to γ-Valerolactone under Ambient Conditions. *Mol. Catal.* **2019**, *475* (1), 110478. https://doi.org/10.1016/j.mcat.2019.110478.

(21) Shams, S.; Ahmad, W.; Memon, A. H.; Wei, Y.; Yuan, Q.; Liang, H. Facile Synthesis of Laccase Mimic Cu/H 3 BTC MOF for Efficient Dye Degradation and Detection of Phenolic Pollutants. *RSC Adv.* **2019**, *9* (70), 40845–40854. https://doi.org/10.1039/C9RA07473B.

(22) Li, X.; Li, D.; Zhang, Y.; Lv, P.; Feng, Q.; Wei, Q. Encapsulation of Enzyme by Metal-Organic Framework for Single-Enzymatic Biofuel Cell-Based Self-Powered Biosensor. *Nano Energy* **2020**, *68* (November 2019), 104308. https://doi.org/10.1016/j.nanoen.2019.104308.

(23) Ashoka Sahadevan, S.; Monni, N.; Oggianu, M.; Abhervé, A.; Marongiu, D.; Saba, M.; Mura, A.; Bongiovanni, G.; Mameli, V.; Cannas, C.; Avarvari, N.; Quochi, F.; Mercuri, M.

L. Heteroleptic NIR-Emitting Yb III /Anilate-Based Neutral Coordination Polymer Nanosheets for Solvent Sensing. *ACS Appl. Nano Mater.* **2020**, *3* (1), 94–104. https://doi.org/10.1021/acsanm.9b01740.

(24) Mehta, J.; Bhardwaj, N.; Bhardwaj, S. K.; Kim, K. H.; Deep, A. Recent Advances in Enzyme Immobilization Techniques: Metal-Organic Frameworks as Novel Substrates. *Coord. Chem. Rev.* **2016**, *322*, 30–40. https://doi.org/10.1016/j.ccr.2016.05.007.

(25) Lyu, F.; Zhang, Y.; Zare, R. N.; Ge, J.; Liu, Z. One-Pot Synthesis of Protein-Embedded Metal-Organic Frameworks with Enhanced Biological Activities. *Nano Lett.* **2014**, *14* (10), 5761–5765. https://doi.org/10.1021/nl5026419.

(26) Lykourinou, V.; Chen, Y.; Wang, X. Sen; Meng, L.; Hoang, T.; Ming, L. J.; Musselman, R. L.; Ma, S. Immobilization of MP-11 into a Mesoporous Metal-Organic Framework, MP-11@mesoMOF: A New Platform for Enzymatic Catalysis. *J. Am. Chem. Soc.* **2011**, *133* (27), 10382–10385. https://doi.org/10.1021/ja2038003.

(27) Howarth, A. J.; Liu, Y.; Li, P.; Li, Z.; Wang, T. C.; Hupp, J. T.; Farha, O. K. Chemical, Thermal and Mechanical Stabilities of Metal–Organic Frameworks. *Nat. Rev. Mater.* **2016**, *1*, 15018.

(28) Safaei, M.; Foroughi, M. M.; Ebrahimpoor, N.; Jahani, S.; Omidi, A.; Khatami, M. A Review on Metal-Organic Frameworks: Synthesis and Applications. *TrAC Trends Anal. Chem.* **2019**, *118*, 401–425. https://doi.org/10.1016/j.trac.2019.06.007.

(29) Drout, R. J.; Robison, L.; Farha, O. K. Catalytic Applications of Enzymes Encapsulated in Metal–Organic Frameworks. *Coord. Chem. Rev.* **2019**, *381*, 151–160.

\

https://doi.org/10.1016/j.ccr.2018.11.009.

(30) Carucci, C.; Bruen, L.; Gascón, V.; Paradisi, F.; Magner, E. Significant Enhancement of Structural Stability of the Hyperhalophilic ADH from Haloferax Volcanii via Entrapment on Metal Organic Framework Support. *Langmuir* **2018**, *34* (28), 8274–8280. https://doi.org/10.1021/acs.langmuir.8b01037.

(31) Majewski, M. B.; Howarth, A. J.; Li, P.; Wasielewski, M. R.; Hupp, J. T.; Farha, O. K. Enzyme Encapsulation in Metal-Organic Frameworks for Applications in Catalysis. *CrystEngComm* **2017**, *19* (29), 4082–4091. https://doi.org/10.1039/c7ce00022g.

(32) Xia, H.; Li, N.; Zhong, X.; Jiang, Y. Metal-Organic Frameworks: A Potential Platform for Enzyme Immobilization and Related Applications. *Front. Bioeng. Biotechnol.* **2020**, *8* (June), 1–16. https://doi.org/10.3389/fbioe.2020.00695.

(33) Liang, W.; Xu, H.; Carraro, F.; Maddigan, N. K.; Li, Q.; Bell, S. G.; Huang, D. M.; Tarzia, A.; Solomon, M. B.; Amenitsch, H.; Vaccari, L.; Sumby, C. J.; Falcaro, P.; Doonan, C. J. Enhanced Activity of Enzymes Encapsulated in Hydrophilic Metal-Organic Frameworks. *J. Am. Chem. Soc.* **2019**. https://doi.org/10.1021/jacs.8b10302.

(34) Li, Z.; Xia, H.; Li, S.; Pang, J.; Zhu, W.; Jiang, Y. In Situ Hybridization of Enzymes and Their Metal-Organic Framework Analogues with Enhanced Activity and Stability by Biomimetic Mineralisation. *Nanoscale* **2017**, *9* (40), 15298–15302. https://doi.org/10.1039/c7nr06315f.

(35) Zhao, M.; Li, Y.; Ma, X.; Xia, M.; Zhang, Y. Adsorption of Cholesterol Oxidase and Entrapment of Horseradish Peroxidase in Metal-Organic Frameworks for the Colorimetric

\

Biosensing of Cholesterol. *Talanta* **2019**, *200* (December 2018), 293–299. https://doi.org/10.1016/j.talanta.2019.03.060.

(36) Lee, Y.-R.; Kim, J.; Ahn, W.-S. Synthesis of Metal-Organic Frameworks: A Mini Review. *Korean J. Chem. Eng.* **2013**, *30* (9), 1667–1680. https://doi.org/10.1007/s11814-013-0140-6.

(37) Sanchez-Sanchez, M.; de Asua, I.; Ruano, D.; Diaz, K. Direct Synthesis, Structural Features, and Enhanced Catalytic Activity of the Basolite F300-like Semiamorphous Fe-BTC Framework. *Cryst. Growth Des.* **2015**, *15* (9), 4498–4506. https://doi.org/10.1021/acs.cgd.5b00755.

(38) Gascón, V.; Carucci, C.; Jiménez, M. B.; Blanco, R. M.; Sánchez-Sánchez, M.; Magner, E. Rapid In Situ Immobilization of Enzymes in Metal-Organic Framework Supports under Mild Conditions. *ChemCatChem* **2017**, *9* (7), 1182–1186. https://doi.org/10.1002/cctc.201601342.

(39) Kida, K.; Okita, M.; Fujita, K.; Tanaka, S.; Miyake, Y. Formation of High Crystalline ZIF-8 in an Aqueous Solution. *CrystEngComm* **2013**, *15* (9), 1794–1801. https://doi.org/10.1039/c2ce26847g.

(40) Tan, J. C.; Bennett, T. D.; Cheetham, A. K. Chemical Structure, Network Topology, and Porosity Effects on the Mechanical Properties of Zeolitic Imidazolate Frameworks. *Proc. Natl. Acad. Sci. U. S. A.* **2010**, *107* (22), 9938–9943. https://doi.org/10.1073/pnas.1003205107.

(41) Serhan, M.; Sprowls, M.; Jackemeyer, D.; Long, M.; Perez, I. D.; Maret, W.; Tao, N.;

\

Forzani, E. Total Iron Measurement in Human Serum with a Smartphone. *AIChE Annu. Meet. Conf. Proc.* **2019**, *2019-Novem*. https://doi.org/10.1039/x0xx00000x.

(42) Liang, W.; Ricco, R.; Maddigan, N. K.; Dickinson, R. P.; Xu, H.; Li, Q.; Sumby, C. J.; Bell, S. G.; Falcaro, P.; Doonan, C. J. Control of Structure Topology and Spatial Distribution of Biomacromolecules in Protein@ZIF-8 Biocomposites. *Chem. Mater.* **2018**, *30* (3), 1069–1077. https://doi.org/10.1021/acs.chemmater.7b04977.

(43) Zucca, P.; Cocco, G.; Sollai, F.; Sanjust, E. Fungal Laccases as Tools for Biodegradation of Industrial Dyes. *Biocatalysis* **2016**, *1* (1), 82–108. https://doi.org/10.1515/boca-2015-0007.

(44) Riva, S. Laccases: Blue Enzymes for Green Chemistry. *Trends Biotechnol.* **2006**, *24* (5), 219–226. https://doi.org/10.1016/j.tibtech.2006.03.006.

(45) Kersten, P. J.; Kalyanaraman, B.; Hammel, K. E.; Reinhammar, B.; Kirk, T. K. Comparison of Lignin Peroxidase, Horseradish Peroxidase and Laccase in the Oxidation of Methoxybenzenes. *Biochem. J.* **1990**, *268* (2), 475–480. https://doi.org/10.1042/bj2680475.

(46) Bertrand, B.; Martínez-Morales, F.; Trejo-Hernández, M. R. Upgrading Laccase Production and Biochemical Properties: Strategies and Challenges. *Biotechnol. Prog.* **2017**, *33* (4), 1015–1034. https://doi.org/10.1002/btpr.2482.

(47) Tocco, D.; Carucci, C.; Monduzzi, M.; Salis, A.; Sanjust, E. Recent Developments in the Delignification and Exploitation of Grass Lignocellulosic Biomass. *ACS Sustain. Chem. Eng.* **2021**, *9* (6), 2412–2432. https://doi.org/10.1021/acssuschemeng.0c07266.

\

(48) Unuofin, J. O. Treasure from Dross: Application of Agroindustrial Wastes-Derived Thermo-Halotolerant Laccases in the Simultaneous Bioscouring of Denim Fabric and Decolorization of Dye Bath Effluents. *Ind. Crops Prod.* **2020**, *147* (February), 112251. https://doi.org/10.1016/j.indcrop.2020.112251.

(49) Prasetyo, E. N.; Semlitsch, S.; Nyanhongo, G. S.; Lemmouchi, Y.; Guebitz, G. M. Laccase Oxidation and Removal of Toxicants Released during Combustion Processes. *Chemosphere* **2016**, *144*, 652–660. https://doi.org/10.1016/j.chemosphere.2015.07.082.

(50) Zucca, P.; Sanjust, E. Inorganic Materials as Supports for Covalent Enzyme Immobilization: Methods and Mechanisms. *Molecules* **2014**, *19* (9), 14139–14194. https://doi.org/10.3390/molecules190914139.

(51) Wong, D. W. S. Structure and Action Mechanism of Ligninolytic Enzymes. *Appl. Biochem. Biotechnol.* **2009**, *157* (2), 174–209. https://doi.org/10.1007/s12010-008-8279-z.

(52) Rico, A.; Rencoret, J.; del Río, J. C.; Martínez, A. T.; Gutiérrez, A. Pretreatment with Laccase and a Phenolic Mediator Degrades Lignin and Enhances Saccharification of Eucalyptus Feedstock. *Biotechnol. Biofuels* **2014**, *7* (1), 6. https://doi.org/10.1186/1754-6834-7-6.

(53) Asgher, M.; Wahab, A.; Bilal, M.; Iqbal, H. M. N. Delignification of Lignocellulose Biomasses by Alginate–Chitosan Immobilized Laccase Produced from Trametes Versicolor IBL-04. *Waste and Biomass Valorization* **2018**, *9* (11), 2071–2079. https://doi.org/10.1007/s12649-017-9991-0.

(54) Naseri, M.; Pitzalis, F.; Carucci, C.; Medda, L.; Fotouhi, L.; Magner, E.; Salis, A. Lipase

\

and Laccase Encapsulated on Zeolite Imidazolate Framework: Enzyme Activity and Stability from Voltammetric Measurements. *ChemCatChem* **2018**, *10* (23), 5425–5433. https://doi.org/10.1002/cctc.201801293.

(55) Gascón, V.; Jiménez, M. B.; Blanco, R. M.; Sanchez-Sanchez, M. Semi-Crystalline Fe-BTC MOF Material as an Efficient Support for Enzyme Immobilization. *Catal. Today* **2018**, *304* (October 2017), 119–126. https://doi.org/10.1016/j.cattod.2017.10.022.

(56) Marzorati, M.; Danieli, B.; Haltrich, D.; Riva, S. Selective Laccase-Mediated Oxidation of Sugars Derivatives. *Green Chem.* **2005**, *7* (5), 310–315. https://doi.org/10.1039/b416668j.

(57) Baldrian, P. Fungal Laccases – Occurrence and Properties. *FEMS Microbiol. Rev.* **2006**, *30* (2), 215–242. https://doi.org/10.1111/j.1574-4976.2005.00010.x.

(58) Gianfreda, L.; Xu, F.; Bollag, J. M. Laccases: A Useful Group of Oxidoreductive Enzymes. *Bioremediat. J.* **1999**, *3* (1), 1–26. https://doi.org/10.1080/10889869991219163.

(59) Wei, T. H.; Wu, S. H.; Huang, Y. Da; Lo, W. S.; Williams, B. P.; Chen, S. Y.; Yang, H. C.; Hsu, Y. S.; Lin, Z. Y.; Chen, X. H.; Kuo, P. E.; Chou, L. Y.; Tsung, C. K.; Shieh, F. K. Rapid Mechanochemical Encapsulation of Biocatalysts into Robust Metal–Organic Frameworks. *Nat. Commun.* **2019**, *10* (1), 1–8. https://doi.org/10.1038/s41467-019-12966-0.

(60) Liu, X.; Qi, W.; Wang, Y.; Su, R.; He, Z. A Facile Strategy for Enzyme Immobilization with Highly Stable Hierarchically Porous Metal-Organic Frameworks. *Nanoscale* **2017**, *9* (44), 17561–17570. https://doi.org/10.1039/c7nr06019j.

\

(61) Autie-Castro, G.; Autie, M. A.; Rodríguez-Castellón, E.; Aguirre, C.; Reguera, E. Cu-BTC and Fe-BTC Metal-Organic Frameworks: Role of the Materials Structural Features on Their Performance for Volatile Hydrocarbons Separation. *Colloids Surfaces A Physicochem. Eng. Asp.* **2015**, *481*, 351–357. https://doi.org/10.1016/j.colsurfa.2015.05.044.

(62) Seo, Y. K.; Yoon, J. W.; Lee, J. S.; Lee, U. H.; Hwang, Y. K.; Jun, C. H.; Horcajada, P.; Serre, C.; Chang, J. S. Large Scale Fluorine-Free Synthesis of Hierarchically Porous Iron(III) Trimesate MIL-100(Fe) with a Zeolite MTN Topology. *Microporous Mesoporous Mater.* **2012**, *157*, 137–145. https://doi.org/10.1016/j.micromeso.2012.02.027.

(63) Hikov, T.; Schröder, C. A.; Cravillon, J.; Wiebcke, M.; Huber, K. In Situ Static and Dynamic Light Scattering and Scanning Electron Microscopy Study on the Crystallization of the Dense Zinc Imidazolate Framework ZIF-Zni. *Phys. Chem. Chem. Phys.* **2012**, *14* (2), 511–521. https://doi.org/10.1039/c1cp22855b.

(64) Huang, S.; Yang, K.-L.; Liu, X.-F.; Pan, H.; Zhang, H.; Yang, S. MIL-100(Fe)-Catalyzed Efficient Conversion of Hexoses to Lactic Acid. *RSC Adv.* **2017**, *7* (10), 5621–5627. https://doi.org/10.1039/C6RA26469G.

(65) Yang, Y.; Bai, Y.; Zhao, F.; Yao, E.; Yi, J.; Xuan, C.; Chen, S. Effects of Metal Organic Framework Fe-BTC on the Thermal Decomposition of Ammonium Perchlorate. *RSC Adv.* **2016**, *6* (71), 67308–67314. https://doi.org/10.1039/C6RA12634K.

(66) Cravillon, J.; Nayuk, R.; Springer, S.; Feldhoff, A.; Huber, K.; Wiebcke, M. Controlling Zeolitic Imidazolate Framework Nano- and Microcrystal Formation: Insight into Crystal Growth by Time-Resolved In Situ Static Light Scattering. *Chem. Mater.* **2011**, *23* (8), 2130–

\

2141. https://doi.org/10.1021/cm103571y.

(67) James, J. B.; Lin, Y. S. Kinetics of ZIF-8 Thermal Decomposition in Inert, Oxidizing, and Reducing Environments. *J. Phys. Chem. C* **2016**, *120* (26), 14015–14026. https://doi.org/10.1021/acs.jpcc.6b01208.

(68) Park, K. S.; Ni, Z.; Côté, A. P.; Choi, J. Y.; Huang, R.; Uribe-Romo, F. J.; Chae, H. K.; O'Keeffe, M.; Yaghi, O. M. Exceptional Chemical and Thermal Stability of Zeolitic Imidazolate Frameworks. *Proc. Natl. Acad. Sci. U. S. A.* **2006**, *103* (27), 10186–10191. https://doi.org/10.1073/pnas.0602439103.

(69) Majano, G.; Ingold, O.; Yulikov, M.; Jeschke, G.; Pérez-Ramírez, J. Room-Temperature Synthesis of Fe–BTC from Layered Iron Hydroxides: The Influence of Precursor Organisation. *CrystEngComm* **2013**, *15* (46), 9885. https://doi.org/10.1039/c3ce41366g.

(70) Lv, H.; Zhao, H.; Cao, T.; Qian, L.; Wang, Y.; Zhao, G. Efficient Degradation of High Concentration Azo-Dye Wastewater by Heterogeneous Fenton Process with Iron-Based Metal-Organic Framework. *J. Mol. Catal. A Chem.* **2015**, *400* (May 2015), 81–89. https://doi.org/10.1016/j.molcata.2015.02.007.

(71) Pangkumhang, B.; Jutaporn, P.; Sorachoti, K.; Khamdahsag, P.; Tanboonchuy, V. Applicability of Iron (III) Trimesic (Fe-BTC) to Enhance Lignin Separation from Pulp and Paper Wastewater. *Sains Malaysiana* **2019**, *48* (1), 199–208. https://doi.org/10.17576/jsm-2019-4801-23.

(72) Rafiei, S.; Tangestaninejad, S.; Horcajada, P.; Moghadam, M.; Mirkhani, V.; Mohammadpoor-Baltork, I.; Kardanpour, R.; Zadehahmadi, F. Efficient Biodiesel

\

Production Using a Lipase@ZIF-67 Nanobioreactor. *Chem. Eng. J.* **2018**, *334* (October 2017), 1233–1241. https://doi.org/10.1016/j.cej.2017.10.094.

(73) Liu, J.; He, J.; Wang, L.; Li, R.; Chen, P.; Rao, X.; Deng, L.; Rong, L.; Lei, J. NiO-PTA Supported on ZIF-8 as a Highly Effective Catalyst for Hydrocracking of Jatropha Oil. *Sci. Rep.* **2016**, *6* (1), 23667. https://doi.org/10.1038/srep23667.

(74) Nasihat Sheno, N.; Farhadi, S.; Maleki, A.; Hamidi, M. A Novel Approach for the Synthesis of Phospholipid Bilayer-Coated Zeolitic Imidazolate Frameworks: Preparation and Characterization as a PH-Responsive Drug Delivery System. *New J. Chem.* **2019**, *43* (4), 1956–1963. https://doi.org/10.1039/C8NJ04715D.

(75) Xia, Q.; Wang, H.; Huang, B.; Yuan, X.; Zhang, J.; Zhang, J.; Jiang, L.; Xiong, T.; Zeng, G. State-of-the-Art Advances and Challenges of Iron-Based Metal Organic Frameworks from Attractive Features, Synthesis to Multifunctional Applications. *Small* **2019**, *15* (2), 1–25. https://doi.org/10.1002/smll.201803088.

(76) Oveisi, A. R.; Khorramabadi-Zad, A.; Daliran, S. Iron-Based Metal-Organic Framework, Fe(BTC): An Effective Dual-Functional Catalyst for Oxidative Cyclization of Bisnaphthols and Tandem Synthesis of Quinazolin-4(3H)-Ones. *RSC Adv.* **2016**, *6* (2), 1136–1142. https://doi.org/10.1039/c5ra19013d.

(77) Salazar-Aguilar, A. D.; Vega, G.; Casas, J. A.; Vega-Díaz, S. M.; Tristan, F.; Meneses-Rodríguez, D.; Belmonte, M.; Quintanilla, A. Direct Hydroxylation of Phenol to Dihydroxybenzenes by H2O2 and Fe-Based Metal-Organic Framework Catalyst at Room Temperature. *Catalysts* **2020**, *10* (2), 1–14. https://doi.org/10.3390/catal10020172.

\

(78) Li, X.; Lachmanski, L.; Safi, S.; Sene, S.; Serre, C.; Grenèche, J. M.; Zhang, J.; Gref, R. New Insights into the Degradation Mechanism of Metal-Organic Frameworks Drug Carriers. *Sci. Rep.* **2017**, *7* (1), 1–11. https://doi.org/10.1038/s41598-017-13323-1.

(79) Velásquez-Hernández, M. D. J.; Ricco, R.; Carraro, F.; Limpoco, F. T.; Linares-Moreau, M.; Leitner, E.; Wiltsche, H.; Rattenberger, J.; Schröttner, H.; Frühwirt, P.; Stadler, E. M.; Gescheidt, G.; Amenitsch, H.; Doonan, C. J.; Falcaro, P. Degradation of ZIF-8 in Phosphate Buffered Saline Media. *CrystEngComm* **2019**, *21* (31), 4538–4544. https://doi.org/10.1039/c9ce00757a.

(80) Luzuriaga, M. A.; Benjamin, C. E.; Gaertner, M. W.; Lee, H.; Herbert, F. C.; Mallick, S.; Gassensmith, J. J. ZIF-8 Degrades in Cell Media, Serum, and Some—but Not All—Common Laboratory Buffers. *Supramol. Chem.* **2019**, *31* (8), 485–490. https://doi.org/10.1080/10610278.2019.1616089.

(81) Du, Y.; Gao, J.; Zhou, L.; Ma, L.; He, Y.; Zheng, X.; Huang, Z.; Jiang, Y. MOF-Based Nanotubes to Hollow Nanospheres through Protein-Induced Soft-Templating Pathways. *Adv. Sci.* **2019**, *6* (6), 6–11. https://doi.org/10.1002/advs.201801684.

(82) Gökgöz, M.; Altinok, H. Immobilization of Laccase on Polyacrylamide and Polyacrylamide κ Carragennan-Based Semi-Interpenetrating Polymer Networks. *Artif. Cells, Blood Substitutes, Biotechnol.* **2012**, *40* (5), 326–330. https://doi.org/10.3109/10731199.2012.658469.

(83) Patil, P. D.; Yadav, G. D. Rapid In Situ Encapsulation of Laccase into Metal-Organic Framework Support (ZIF-8) under Biocompatible Conditions. *ChemistrySelect* **2018**, *3*

\

(17), 4669–4675. https://doi.org/10.1002/slct.201702852.

(84) Salis, A.; Svensson, I.; Monduzzi, M.; Solinas, V.; Adlercreutz, P. The Atypical Lipase B from Candida Antarctica Is Better Adapted for Organic Media than the Typical Lipase from Thermomyces Lanuginosa. *Biochim. Biophys. Acta - Proteins Proteomics* **2003**, *1646* (1–2), 145–151. https://doi.org/10.1016/S1570-9639(02)00556-3.

(85) Giardina, P.; Faraco, V.; Pezzella, C.; Piscitelli, A.; Vanhulle, S.; Sannia, G. Laccases: A Never-Ending Story. *Cell. Mol. Life Sci.* **2010**, *67* (3), 369–385. https://doi.org/10.1007/s00018-009-0169-1.

(86) Wan, Y. Y.; Lu, R.; Xiao, L.; Du, Y. M.; Miyakoshi, T.; Chen, C. L.; Knill, C. J.; Kennedy, J. F. Effects of Organic Solvents on the Activity of Free and Immobilised Laccase from Rhus Vernicifera. *Int. J. Biol. Macromol.* **2010**, *47* (4), 488–495. https://doi.org/10.1016/j.ijbiomac.2010.07.003.

(87) Ulu, A. Metal–Organic Frameworks (MOFs): A Novel Support Platform for ASNase Immobilization. *J. Mater. Sci.* **2020**, *55* (14), 6130–6144. https://doi.org/10.1007/s10853-020-04452-6.

(88) Maddigan, N. K.; Linder-Patton, O. M.; Falcaro, P.; Sumby, C. J.; Bell, S. G.; Doonan, C. J. Influence of the Synthesis and Storage Conditions on the Activity of Candida Antarctica Lipase B ZIF-8 Biocomposites. *ACS Appl. Mater. Interfaces* **2021**. https://doi.org/10.1021/acsami.1c04785.